


Original article

Neuropsychiatric systemic lupus erythematosus is associated with a distinct type and shape of cerebral white matter hyperintensities

Francesca Inglese ¹, Myriam G. Jaarsma-Coes¹,
Gerda M. Steup-Beekman^{2,3}, Rory Monahan², Tom Huizinga²,
Mark A. van Buchem¹, Itamar Ronen¹ and Jeroen de Bresser¹

Abstract

Objectives. Advanced white matter hyperintensity (WMH) markers on brain MRI may help reveal underlying mechanisms and aid in the diagnosis of different phenotypes of SLE patients experiencing neuropsychiatric (NP) manifestations.

Methods. In this prospective cohort study, we included a clinically well-defined cohort of 155 patients consisting of 38 patients with NPSLE (26 inflammatory and 12 ischaemic phenotype) and 117 non-NPSLE patients. Differences in 3T MRI WMH markers (volume, type and shape) were compared between patients with NPSLE and non-NPSLE and between patients with inflammatory and ischaemic NPSLE by linear and logistic regression analyses corrected for age, sex and intracranial volume.

Results. Compared with non-NPSLE [92% female; mean age 42 (13) years], patients with NPSLE [87% female; mean age 40 (14) years] showed a higher total WMH volume [B (95%-CI): 0.46 (0.07 ↔ 0.86); $P=0.021$], a higher periventricular/confluent WMH volume [0.46 (0.06 ↔ 0.86); $P=0.024$], a higher occurrence of periventricular with deep WMH type [0.32 (0.13 ↔ 0.77); $P=0.011$], a higher number of deep WMH lesions [3.06 (1.21 ↔ 4.90); $P=0.001$] and a more complex WMH shape [convexity: -0.07 (-0.12 ↔ -0.02); $P=0.011$, concavity index: 0.05 (0.01 ↔ 0.08); $P=0.007$]. WMH shape was more complex in inflammatory NPSLE patients [89% female; mean age 39 (15) years] compared with patients with the ischaemic phenotype [83% female; mean age 41 (11) years] [concavity index: 0.08 (0.01 ↔ 0.15); $P=0.034$].

Conclusion. We demonstrated that patients with NPSLE showed a higher periventricular/confluent WMH volume and more complex shape of WMH compared with non-NPSLE patients. This finding was particularly significant in inflammatory NPSLE patients, suggesting different or more severe underlying pathophysiological abnormalities.

Key words: SLE, MRI, brain, white matter hyperintensity

Rheumatology key messages

- Advanced white matter hyperintensity (WMH) markers on brain MRI may aid the diagnosis of different phenotypes of neuropsychiatric SLE (NPSLE).
- NPSLE patients showed a higher periventricular/confluent WMH volume and more complex shape of WMH compared to non-NPSLE patients.
- NPSLE inflammatory patients had a more complex WMH shape compared to NPSLE ischaemic patients.

¹Department of Radiology, ²Department of Rheumatology, Leiden University Medical Center, Leiden and ³Department of Rheumatology, Haaglanden Medical Center, The Hague, The Netherlands

Submitted 14 July 2021; accepted 27 October 2021

Correspondence to: Francesca Inglese, Department of Radiology, Leiden University Medical Center (LUMC), Albinusdreef 2, 2333 ZA, Leiden, The Netherlands. E-mail: f.inglese@lumc.nl

Introduction

SLE patients frequently show central nervous system symptoms. These neuropsychiatric (NP) symptoms are diverse and have different severity and prognostic implications [1]. NP symptoms can be directly attributed to SLE (NPSLE) or can be explained by other aetiologies, such as side effects of medication (non-NPSLE) [2]. In

clinical practice, NPSLE patients are classified based on the suspected underlying pathophysiologic mechanism (inflammatory or ischaemic) to define the therapeutic approach [3]. The inflammatory mechanism is possibly associated with the production of inflammatory mediators and/or the increase of blood-brain barrier or blood-CSF barrier permeability [4]. The ischaemic mechanism is likely caused by the injury of large or small-caliber vessels and/or by immune system activation [4]. One of the major issues in clinical practice is the difficulty in attribution of NP symptoms to SLE [5] due to lack of a sensitive and specific radiological or laboratory biomarkers [3].

Brain MRI is frequently used in the clinical evaluation of SLE patients experiencing NP events [6], mainly to exclude other diseases. Common brain MRI abnormalities in patients with NPSLE and non-NPSLE are white matter hyperintensities (WMH) [7–11]. A previous study has shown that NPSLE patients with an inflammatory phenotype tend to have the highest volume of WMH [12]. However, WMH volume alone does not differentiate between NPSLE phenotypes sufficiently. Recently introduced more advanced quantitative WMH markers, such as WMH type and shape, may aid in unravelling relevant aetiological and even prognostic information in patients with (NP)SLE [13–17]. In other diseases, such as cerebral small vessel disease based on arteriolosclerosis, WMH shape markers were associated with an increased mortality and increased risk of stroke [17]. In our study we investigated the differences in these advanced structural WMH markers in patients with different phenotypes of NPSLE.

Materials and methods

Patient population

We have included SLE patients with a suspicion of NP involvement who are referred to the Leiden University Medical Center (LUMC), which is the national referral centre for SLE patients with NP symptoms. Patients are invited to the clinic for a one-day visit and undergo a standardized evaluation that includes a combination of multidisciplinary medical assessments and extensive complementary tests including a brain MRI scan [5]. After this evaluation, a multidisciplinary consensus meeting takes place in order to decide whether the NP events are attributable to SLE. In particular, time between diagnosis of SLE and onset of NP symptoms, type of symptoms and favouring factors or alternative diagnoses are used to define the attribution to SLE [18, 19]. NPSLE diagnosis is very strict as only patients with symptoms severe enough to require treatment other than supportive treatment are diagnosed with NPSLE. In case of attribution of the NP symptoms to SLE, a consensus is reached regarding the suspected underlying pathophysiology of NPSLE: inflammatory or ischaemic [20]. This determination of phenotype is made after evaluation of radiological, serological and clinical data. In the presence of signs of inflammation, like

complement consumption and other SLE manifestations, the inflammatory phenotype is assigned. In the presence of signs of ischaemia and/or the antiphospholipid syndrome, the ischaemic phenotype is assigned. Subsequently, therapy is initiated either with immunosuppressant drugs or with anticoagulant therapy, depending on the phenotype attributed [21]. This multidisciplinary diagnostic process was described in detail previously [5, 22].

A total of 216 consecutively recruited patients that visited the clinic between May 2007 and April 2015 were eligible in our study. To be eligible, patients were considered suspected NPSLE and had a signed informed consent. The Leiden-The Hague-Delft ethics committee approved the study (registration number: P07.177).

Clinical variables

Patient clinical information was collected via interview and taken from medical records. For this study, information on sex, age, cardiovascular risk factors (hypertension, smoking, BMI and diabetes) and SLE disease duration was obtained. SLEDAI 2000 (SLEDAI-2K) [23] and Systemic Lupus International Collaborating Clinics/American College of Rheumatology damage index (SDI) [24] were determined for each patient. All clinical variables and MRI scans were obtained on the same day.

MRI protocol

All participants underwent a standardized brain scan on a Philips Achieva 3T MRI scanner (Philips Healthcare, Best, The Netherlands) equipped with a body transmit RF coil and an 8-Channel receive head coil array. Two sequences of the standard protocol were used for the purpose of our study: a 3D T₁-weighted scan (voxel size = 1.17 × 1.17 × 1.2 mm³; TR/TE = 9.8/4.6 ms) and a fluid-attenuated inversion recovery (FLAIR) scan. A change of the FLAIR protocol occurred in February 2013 (a switch from 2D to 3D acquisition) resulting in 102 patients with a 2D-multislice FLAIR sequence (voxel size = 1.0 × 1.0 × 3.6 mm³; TR/TE/TI = 10000/120/2800 ms) and 53 patients with a 3D FLAIR (voxel size = 1.10 × 1.11 × 0.56 mm³; TR/TE/TI = 4800/576/1650 ms).

Image processing

The FLAIR images were first registered to the 3D-T₁-weighted images, using the Linear Image Registration Tool (FLIRT) from the FMRIB Software Library v5.0 [25, 26]. Then, automatic segmentation of WMH was performed on the registered FLAIR images to generate WMH probability maps using the lesion prediction algorithm, a toolbox of the Lesion Segmentation Toolbox (LST) version 2.0.15 for the statistical parametric mapping software (SPM) version 12 (Wellcome Institute of Neurology, University College London, UK) [27]. A lesion probability threshold of 0.2 was applied to the WMH probability maps to generate WMH masks, subsequently filled on the 3D T₁-weighted images using LST. This

threshold was defined after testing different thresholds between 0.1 and 0.5 on a random selection of patients. The threshold 0.2 visually resulted in the best accuracy of WMH segmentation. WMH volume was calculated using SPM8. The resulting lesion-filled 3D T₁-weighted images were segmented using the CAT12 toolbox from the SPM12 software to determine grey matter, white matter and cerebral-spinal fluid volumes (see Fig. 1) [27]. Total intracranial volume was calculated as the sum of the grey matter, white matter and cerebral-spinal fluid volumes. The next step was to segment the lateral ventricles on the T1 image or on the registered FLAIR using the automated lateral ventricle delineation toolbox (ALVIN) in SPM8 [15, 16]. All MRI images as well as the grey matter, white matter, WMH, lateral ventricles and cerebral-spinal fluid segmentations were visually inspected for segmentation errors and artefacts by two trained researchers (F.I. and M.G.J-C.) and a neuroradiologist with 14 years of experience in brain segmentation (J.dB.), blinded to the clinical data. WMH and lateral ventricular segmentations were manually corrected in case of segmentation errors.

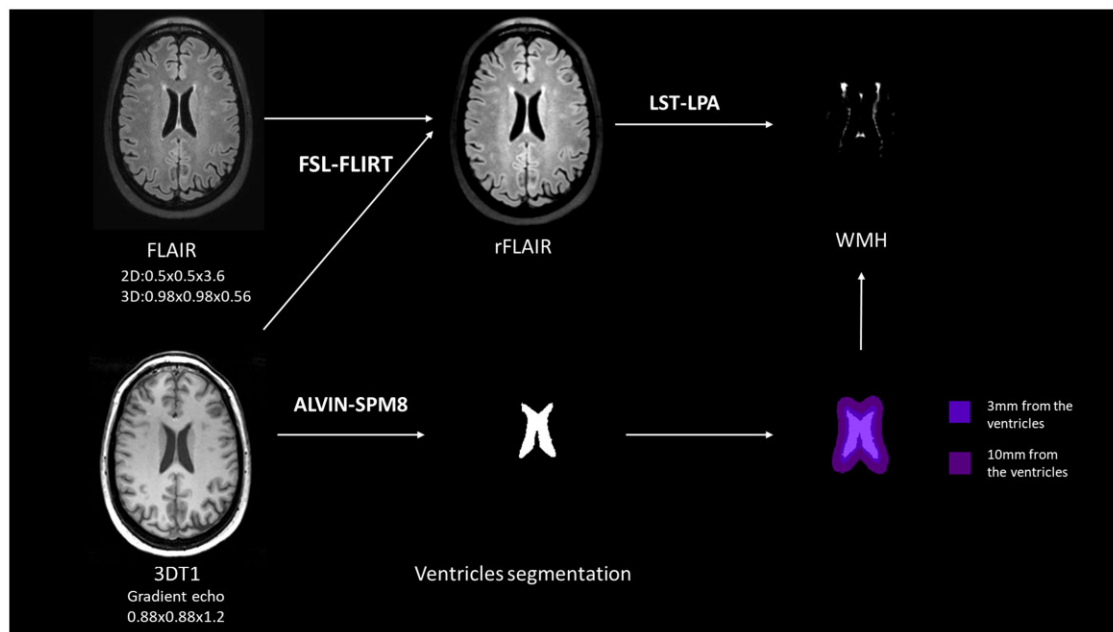
WMH types and shape

Three different types of WMH were assessed: periventricular, confluent and deep WMH. The periventricular WMH type was assigned to WMH within 3 mm,

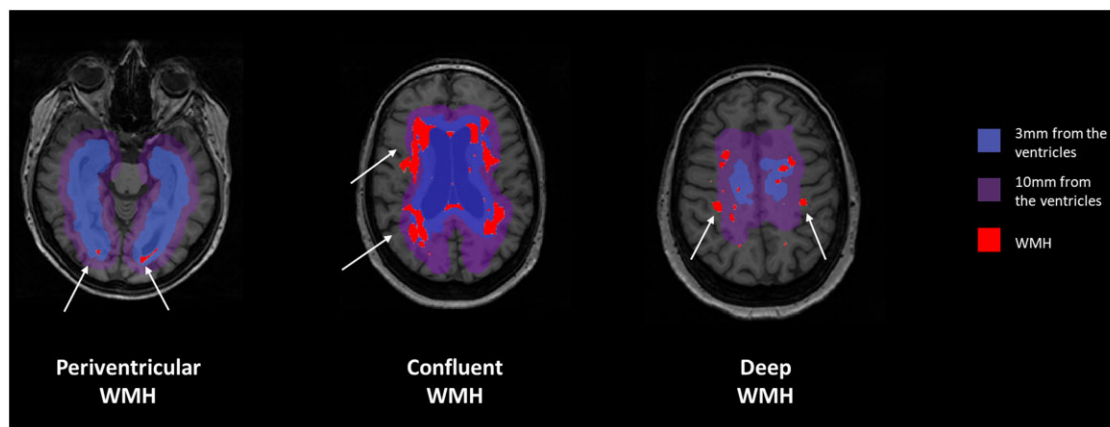
but not extending >10mm from the lateral ventricles into the white matter [28]. The confluent WMH type was assigned to periventricular WMH that extended >10mm into the white matter. The deep WMH type was assigned to WMH that were not in contact with the lateral ventricles (>3mm away from the lateral ventricles) [16]. Figure 2 shows an example of each WMH type.

WMH shape markers were calculated from the WMH segmentation. Solidity, convexity, concavity index and fractal dimension were determined for periventricular/confluent WMH. Eccentricity and fractal dimension were determined for deep WMH. The solidity was calculated by dividing WMH lesion volume by the volume of its convex hull. The convexity was calculated by dividing the convex hull surface area by the lesion's surface area. The concavity index was calculated by reconstructing convex hulls and by determining volume and surface area ratios of lesions [17]. The eccentricity was obtained by dividing the minor axis of a lesion (smallest diameter orthogonal to the major axis) by its major axis (largest diameter of the WMH in three dimensions). The fractal dimension was calculated by using the box counting method [15]. For more details see Supplementary Table S1, available at *Rheumatology* online. Mean or median values per marker were calculated per patient (for details see [15, 16]).

Fig. 1 Pipeline of the white matter hyperintensity marker analysis



FLAIR images were registered to the 3D T₁-weighted images by using the FMRIB's Linear Image Registration Tool (FLIRT) from FMRIB Software Library v5.0 (FSL). White matter hyperintensity segmentations were performed on the registered FLAIR (rFLAIR) using the lesion prediction algorithm (LPA) within the Lesion Segmentation Toolbox (LST) for statistical parametric mapping (SPM12). Lateral ventricular segmentation was performed on the T1 image or on the rFLAIR to the T1 using the toolbox ALVIN in SPM8.

Fig. 2 Definitions of the white matter hyperintensity types

The blue parts show a 3-mm space distance from the lateral ventricles. The purple parts show a 10-mm space distance from the lateral ventricles. In red, WMH lesions are shown. Periventricular WMH were defined as WMH within 3 mm and extending no more than 10 mm from the lateral ventricles into the white matter. Confluent WMH were defined as periventricular WMH that extended from the lateral ventricles to more than 10 mm into the white matter. Deep WMH were defined as WMH that are not in contact with the lateral ventricles (>3 mm away from the ventricles). WMH: white matter hyperintensity.

Statistical analysis

All data were tested for normal distribution by performing Shapiro–Wilk tests and by visualization of histograms and Q–Q plots.

Differences in baseline characteristics between patients with NPSLE and non-NPSLE were determined with χ^2 tests for nominal variables (sex, hypertension, smoking and diabetes), and with unpaired t-tests (age and BMI) or Mann–Whitney U tests (duration of SLE, SLEDAI-2K and SDI) for continuous variables based on their distribution. Differences in total WMH, periventricular WMH, confluent WMH and deep WMH volumes between patients with NPSLE and non-NPSLE were assessed with linear regression analyses corrected for age, sex and total intracranial volume, and expressed as B value (95%-CIs). Differences in prevalence of WMH types between patients with NPSLE and non-NPSLE were determined by logistic regression analysis corrected for sex and age, and expressed as B value (95%-CIs). Differences in number of deep WMH lesions and WMH shape markers between patients with NPSLE and non-NPSLE were assessed through linear regression analysis corrected for sex and age, and expressed as B value (95%-CIs). A secondary analysis was performed to calculate the false discovery rate using the Benjamini & Hochberg method for WMH volumes, types and markers.

Differences in baseline characteristics, WMH volumes, WMH types, number of deep WMH lesions and WMH shape markers between NPSLE patients with an inflammatory phenotype vs patients with an ischaemic phenotype were examined with a similar statistical approach to the comparison between NPSLE and non-NPSLE patients.

For all variables that were non-normally distributed, values were multiplied by 1000 and natural log transformed for the regression analyses. All these exploratory statistical analyses were performed using IBM Statistical Package for the Social Sciences version 25 (IBM corporation, Armonk, NY, USA).

Results

Patient population

A total of 216 patients were eligible in our study. Of these, 61 patients were excluded in total: 28 patients for undefined NPSLE diagnosis or mixed phenotypes, eight patients for misdiagnosis established during follow-up visit, three patients for motion artefacts in the MRI scans, 20 patients for the presence of large brain infarcts (over 1.5 cm) that hinder accurate brain volume measurements and two patients due to the presence of other brain diseases (brain tumour and large arachnoid cyst). After exclusions, a total of 155 patients were included in the present study, of whom 38 patients with NPSLE (26 with inflammatory phenotype and 12 with ischaemic phenotype) and 117 patients with non-NPSLE.

Differences in WMH markers between patients with NPSLE and patients with non-NPSLE

Table 1 shows the characteristics of the patients with NPSLE [$n=38$; 87% female; mean age 40 (14) years] and patients with non-NPSLE [$n=117$; 92% female; mean age 42 (13) years]. Compared with patients with non-NPSLE, patients with NPSLE showed a significantly higher SLEDAI-2K ($P=0.002$) and SDI score ($P=0.045$),

TABLE 1 Characteristics of the patient population

	NPSLE (n = 38)	non-NPSLE (n = 117)	P-value
Female	33 (87%)	108 (92%)	0.307
Age in years	40 (14)	42 (13)	0.351
Cardiovascular risk factors			
Hypertension	16 (42%)	39 (33%)	0.326
Current smoking	5 (13%)	16 (14%)	0.720
BMI	25 (5)	25 (4)	0.990
Diabetes	3 (7%)	6 (5%)	0.626
SLE indexes			
Duration of SLE, years	6 (8)	8 (8)	0.083
SLEDAI-2K	8 (8)	4 (4)	0.002*
SDI	1.1 (1.1)	0.8 (1.1)	0.045*

Sex, age, cardiovascular risk factors and SLE damage indexes are shown. Data are represented as *n* (percentage) or means (s.d.). SDI: systemic lupus international collaborating clinics damage index; SLEDAI-2K: SLEDAI 2000. * $P < 0.05$.

TABLE 2 White matter hyperintensity volumes, types and shape markers.

	NPSLE (n = 38)	Non-NPSLE (n = 117)	NPSLE vs non-NPSLE [B (95%-CI)]
WMH volumes ml			
Total WMH volume	1.59 (0.19-20.40)	1.00 (0.28-6.43)	0.46 (0.07, 0.86)*
Periventricular/confluent WMH volume	1.56 (0.18-17.23)	1.00 (0.25-6.37)	0.46 (0.06, 0.86)*
Deep WMH volume	0.14 (0.02-1.35)	0.12 (0.02-1.05)	0.36 (-0.26, 0.98)
WMH types			
Periventricular	29 (76%)	98 (84%)	1.91 (0.71, 5.16)
Periventricular with deep	17 (45%)	33 (28%)	0.32 (0.13, 0.77)*
Confluent with deep ^a	9 (24%)	19 (16%)	0.52 (0.19, 1.42)
Number of deep WMH	5.21 (8.13)	2.46 (4.50)	3.06 (1.21, 4.90)*
WMH shape markers			
<i>Periventricular/Confluent WMH</i>			
Solidity	0.19 (0.20-0.89)	0.55 (0.19-0.93)	0.01 (-0.20, 0.22)
Convexity	0.99 (0.87-1.20)	1.04 (0.92-1.30)	-0.07 (-0.12, -0.02)*
Concavity index	1.06 (0.96-1.29)	1.04 (0.96-1.16)	0.05 (0.01, 0.08)*
Fractal dimension	1.47 (0.27)	1.41 (0.22)	0.08 (-0.00, 0.16)
<i>Deep WMH</i>			
Eccentricity	0.44 (0.10)	0.45 (0.15)	-0.00 (-0.07, 0.07)
Fractal dimension	1.79 (1.50-1.99)	1.80 (1.47-2.06)	0.01 (-0.05, 0.07)

White matter hyperintensity (WMH) volumes in ml are shown as medians (10–90 percentiles). WMH types prevalence and numbers are shown as *n* (percentage) or means (s.d.). WMH shape markers are shown as means (s.d.) in case of normally distributed variables, or medians (10–90 percentiles) in case of non-normally distributed variables. For the shape analyses of deep WMH, 78 patients were included. The remaining patients did not have deep WMH. Comparisons between the two groups are calculated through linear or logistic regression analysis corrected for sex and age and for the volume comparison also corrected for total intracranial volume. Results are expressed as B or exp B values (95%-CIs). Non-normally distributed variables were multiplied by 1000 and then natural log transformed before the linear regression analysis. ^aDeep WMH are present in all patients with confluent WMH. * $P < 0.05$.

representing a higher disease activity and more irreversible damage, respectively. No between-group differences were found in cardiovascular risk factors (all $P > 0.05$). Additional clinical variables are shown in [Supplementary Tables S2 and S3](#), available at [Rheumatology](#) online.

Patients with NPSLE showed a higher total WMH volume [B (95%-CI): 0.46 (0.07, 0.86); $P = 0.021$] and

periventricular/confluent WMH volume [B (95%-CI): 0.46 (0.06, 0.86); $P = 0.024$] compared with patients with non-NPSLE. There was no statistically significant difference in deep WMH volume [B (95%-CI): 0.36 (-0.26, 0.98); $P = 0.25$] between the patients with NPSLE and patients with non-NPSLE ([Table 2](#)).

The periventricular with deep WMH type was more common in patients with NPSLE compared with patients

TABLE 3 Characteristics of the inflammatory and ischaemic NPSLE population

	NPSLE inflammatory (<i>n</i> = 26)	NPSLE ischaemic (<i>n</i> = 12)	<i>P</i> -value
Female	23 (89%)	10 (83%)	0.664
Age in years	39 (15)	41 (11)	0.581
Cardio-vascular risk factors			
Hypertension	11 (42%)	5 (42%)	0.970
Current smoking	3 (12%)	2 (17%)	0.666
BMI	24 (5)	26 (5)	0.274
Diabetes	1 (3%)	2 (15%)	0.154
SLE indexes			
Duration of SLE, years	4 (6)	10 (10)	0.012*
SLEDAI-2K	10 (9)	4 (3)	0.030*
SDI	1.0 (1.1)	1.3 (1.0)	0.185

Sex, age, cardio-vascular risk factors and SLE damage indexes are shown. Data are represented as *n* (percentage) or means (s.d.). SDI: systemic lupus international collaborating clinics damage index; SLEDAI-2K: SLEDAI 2000. **P* < 0.05.

with non-NPSLE [B (95%-CI): 0.32 (0.13, 0.77); *P* = 0.011]. Periventricular WMH and confluent with deep WMH showed no differences between groups (*P* > 0.05). Patients with NPSLE showed a higher number of deep WMH lesions [B (95%-CI): 3.06 (1.21, 4.90); *P* = 0.001] compared with non-NPSLE patients (Table 2).

NPSLE patients showed a more complex shape of periventricular/confluent WMH compared with non-NPSLE patients [lower convexity: B (95%-CI): -0.07 (-0.12 to -0.02); *P* = 0.011, higher concavity index: B (95%-CI): 0.05 (0.01, 0.08); *P* = 0.007, and a higher fractal dimension without reaching statistical significance: B (95%-CI): 0.08 (-0.00, 0.16); *P* = 0.052]. There was no difference between NPSLE patients and non-NPSLE patients in the shape of deep WMH (*P* > 0.05) (Table 2). Differences did not attenuate when correcting for false discovery rate.

Differences in WMH markers between patients with an inflammatory phenotype and those with an ischaemic phenotype of NPSLE

Table 3 shows the characteristics of the patients with NPSLE (*n* = 38) subdivided into the inflammatory [*n* = 26; 89% female; mean age 39 (15) years] and ischaemic phenotype [*n* = 12; 83% female; mean age 41 (11) years]. Patients with the inflammatory phenotype of NPSLE showed a significantly shorter disease duration (*P* = 0.012) and a higher SLEDAI-2K score (*P* = 0.030) compared with patients with the ischaemic phenotype of NPSLE. No between-group differences were found in cardiovascular risk factors (*P* > 0.05).

Patients with inflammatory phenotype of NPSLE showed no significant differences in total WMH volume, periventricular/confluent WMH volume, or WMH types compared with patients with an ischaemic phenotype of NPSLE (*P* > 0.05) (Table 4). Although the differences were not significant, the values of the deep WMH volume and number of deep WMH seems to be higher in the inflammatory group. Furthermore, patients with the inflammatory phenotype of NPSLE did show a more

complex shape of periventricular/confluent WMH [higher concavity index: B (95%-CI): 0.08 (0.01, 0.15); *P* = 0.034] compared with patients with the ischaemic phenotype of NPSLE. This result became not significant in secondary analysis when correcting for false discovery rate.

Discussion

In our exploratory analyses, we found that compared with non-NPSLE patients, patients with NPSLE showed a higher total WMH volume, a higher periventricular/confluent WMH volume, a higher occurrence of a periventricular with deep WMH type, a higher number of deep WMH lesions and a more complex WMH shape (lower convexity and higher concavity index). Furthermore, patients with an inflammatory phenotype of NPSLE had a more complex shape of periventricular/confluent WMH compared with patients with an ischaemic phenotype (higher concavity index).

In our exploratory study, we stratified WMH in terms of a periventricular/confluent WMH and a deep WMH type and we showed a higher periventricular/confluent WMH volume in NPSLE patients compared with non-NPSLE patients. Previous studies have already shown that NPSLE patients have a higher WMH volume compared with non-NPSLE patients [12, 29], which is in line with our results. However, the volume of different types of WMH has not been assessed in previous studies on NPSLE. Our findings suggest that patients with NPSLE may have a specific preferential location of involvement of WMH. It is currently impossible to attribute these findings to differences in underlying pathophysiological changes, as no previous histopathological studies are available addressing different types of WMH in NPSLE. Based on the significantly higher prevalence of this type of lesions in NPSLE, we suggest that the preferential periventricular/confluent type of WMH in NPSLE is an underlying structural correlate of the neuropsychiatric manifestations in NPSLE. It is important to consider that WMH related to ageing-related types of cerebral small

TABLE 4 White matter hyperintensity volumes, types and shape markers

	NPSLE inflammatory (n = 26)	NPSLE ischaemic (n = 12)	NPSLE inflammatory vs NPSLE ischaemic [B (95%-CI)]
WMH volume ml			
Total WMH volume	1.59 (0.18-20.84)	1.61 (0.24-9.97)	0.49 (-0.39, 1.38)
Periventricular/confluent WMH volume	1.56 (1.48-19.40)	1.60 (0.20-9.46)	0.52 (-0.35, 1.39)
Deep WMH volume	0.27 (0.02-1.92)	0.11 (0.01-0.52)	0.82 (-0.35, 2.00)
WMH types			
Periventricular	20 (77%)	9 (75%)	1.19 (0.19, 7.37)
Periventricular with deep	11 (42%)	6 (50%)	2.10 (0.32, 13.24)
Confluent with deep ^a	6 (23%)	3 (25%)	0.84 (0.14, 5.18)
Number of deep WMH	6.08 (9.31)	3.33 (4.44)	3.90 (-0.68, 8.49)
WMH shape markers			
<i>Periventricular/Confluent WMH</i>			
Solidity	0.52 (0.17-0.90)	0.68 (0.26-0.91)	-0.35 (-0.72, 0.01)
Convexity	0.98 (0.83-1.22)	1.03 (0.88-1.24)	-0.03 (-0.12, 0.06)
Concavity index	1.08 (0.98-1.35)	1.04 (0.96-1.21)	0.08 (0.01, 0.15)
Fractal dimension	1.48 (0.28)	1.44 (0.23)	0.08 (-0.09, 0.25)
<i>Deep WMH</i>			
Eccentricity	0.44 (0.10)	0.44 (0.12)	-0.01 (-0.10, 0.09)
Fractal dimension	1.77 (1.44-1.98)	1.79 (1.52-2.04)	-0.01 (-0.10, 0.08)

White matter hyperintensity (WMH) volumes in ml are shown as medians (10–90 percentiles). WMH types prevalence's and numbers are shown as *n* (percentage) or means (s.d.). WMH shape markers are shown as means (s.d.) in case of normally distributed variables, or medians (10–90 percentiles) in case of non-normally distributed variables. For the shape analyses of deep WMH 26 patients were included, because the other patients did not have deep WMH. Comparisons between the two groups are calculated through linear or logistic regression analysis corrected for sex and age and for the volume comparison also corrected for total intracranial volume. Results are expressed as B or exp B values (95%-CIs). Non-normally distributed variables were multiplied by 1000 and then natural log transformed before the linear regression analysis. ^aDeep WMH are present in all patients with confluent WMH. **P* < 0.05.

vessel disease, such as that based on arteriolosclerosis, might also partially overlap with the abnormalities of SLE. This common type of small vessel disease might indeed be the underlying cause of some of the deep WMH found in patients with SLE.

This work is the first to report on WMH shape markers in SLE. Previous studies in other cerebral diseases (such as arteriolosclerosis-based cerebral small vessel disease) have shown that WMH shape markers may provide additional information regarding aetiology and prognosis [13–17]. For example, in cerebral small vessel disease it has been shown that a more complex WMH shape was associated with an increased mortality and an increased risk of stroke [17]. Therefore, a more complex WMH shape might represent more severe underlying brain changes. We showed that NPSLE patients have a more complex shape of periventricular/confluent WMH compared with non-NPSLE patients. It is plausible that a more complex shape of periventricular/confluent WMH in patients with NPSLE represents more severe damage to the brain tissue and may be part of the underlying structural correlates leading to NP manifestations. Additional histopathological data are needed to support this interpretation. Future studies could focus on the prognostic implications of differences in WMH shape in patients with SLE.

We also investigated differences between the inflammatory and ischaemic phenotype of NPSLE in terms of

WMH volume, types and shape. We found that NPSLE patients with an inflammatory phenotype showed a more complex shape of periventricular/confluent WMH compared with patients with the ischaemic phenotype. A previous study already showed that the inflammatory phenotype of NPSLE is associated with more severe other brain abnormalities (lower brain volumes) compared with the ischaemic phenotype [12]. Combining these findings may suggest that a more complex shape of periventricular/confluent WMH represents more severe structural damage to the brain.

Our findings regarding distinct patterns of WMH type and shape in different phenotypes of NPSLE might have diagnostic potential. Together with other diagnostic markers, WMH type and shape might be helpful in diagnosis of a certain phenotype of NPSLE. As such, these markers could also be useful and clinically relevant to improve the diagnostic and treatment decisions in patients with presumed NPSLE.

Strengths of our study include the detailed assessment of both more commonly used markers of WMH (volume) and more novel advanced markers of WMH, specifically types and shape. Furthermore, we included a relatively large, well-defined and well-phenotyped cohort of patients with NPSLE.

The limitations of this study include the relatively lower number of patients with the ischaemic phenotype of NPSLE compared with patients with the inflammatory

phenotype. Even in our relatively large NPSLE patient population, the prevalence of ischaemic patients was low. Excluding patients with brain infarcts bigger than 1.5 cm could have led to selection bias in the group of ischaemic patients and could have contributed to the relatively low number of patients in this group. However, out of the 20 patients excluded for large brain infarcts, only five patients had ischaemic NPSLE. Another limitation could be the use of both 2D and 3D FLAIR MRI scans in our study, which may have introduced small variations in measurements. To limit bias, our image processing pipeline included methods that are relatively robust for differences in MRI sequences and we also performed extensive quality control assessments [30, 31]. Another limitation could be that our centre is a tertiary referral centre for NPSLE, which might limit the external validity of our results to the general SLE population. However, this bias is of less relevance as a (radiological) biomarker is strongly needed especially for the most challenging patients with possible NPSLE.

In conclusion, we showed that patients with NPSLE showed a higher periventricular/confluent WMH volume and more complex shape of WMH compared with non-NPSLE patients. This finding was particularly significant in patients with the inflammatory phenotype of NPSLE, suggesting different or more severe underlying pathophysiological abnormalities. These MRI markers could be discussed during multidisciplinary meetings as they might be useful and clinically relevant to improve the diagnostic and treatment decisions in patients with presumed NPSLE.

Funding: No specific funding was received from any bodies in the public, commercial or not-for-profit sectors to carry out the work described in this article.

Disclosure statement: All authors have declared no conflicts of interest.

Data availability statement

The data underlying this article will be shared on reasonable request to the corresponding author.

Supplementary data

Supplementary data are available at *Rheumatology* online.

References

- Schwartz N, Stock AD, Putterman C. Neuropsychiatric lupus: new mechanistic insights and future treatment directions. *Nat Rev Rheumatol* 2019;15:137–52.
- Ainiala H, Loukkola J, Peltola J, Korpela M, Hietaharju A. The prevalence of neuropsychiatric syndromes in systemic lupus erythematosus. *Neurology* 2001;57:496–500.
- Magro-Checa C, Zirkzee EJ, Beaat-van de Voorde LJJ *et al.* Value of multidisciplinary reassessment in attribution of neuropsychiatric events to systemic lupus erythematosus: prospective data from the Leiden NPSLE cohort. *Rheumatology* 2017;56:1676–83.
- Hanly JG, Kozora E, Beyea SD, Birnbaum J. Review: nervous system disease in systemic lupus erythematosus: current status and future directions. *Arthritis Rheumatol* 2019;71:33–42.
- Zirkzee EJM, Steup-Beekman GM, Van Der Mast RC *et al.* Prospective study of clinical phenotypes in neuropsychiatric systemic lupus erythematosus; multidisciplinary approach to diagnosis and therapy. *J Rheumatol* 2012;39:2118–26.
- Bertsias GK, Ioannidis JPA, Aringer M *et al.* EULAR recommendations for the management of systemic lupus erythematosus with neuropsychiatric manifestations: report of a task force of the EULAR standing committee for clinical affairs. *Ann Rheum Dis* 2010;69:2074–82.
- Govoni M, Bortoluzzi A, Padovan M *et al.* The diagnosis and clinical management of the neuropsychiatric manifestations of lupus. *J Autoimmun* 2016;74:41–72.
- Magro-Checa C, Steup-Beekman GM, Huizinga TW, van Buchem MA, Ronen I. Laboratory and neuroimaging biomarkers in neuropsychiatric systemic lupus erythematosus: where do we stand, where to go? *Front Med* 2018;5:340.
- Luyendijk J, Steens SCA, Ouwendijk WJN *et al.* Neuropsychiatric systemic lupus erythematosus: lessons learned from magnetic resonance imaging. *Arthritis Rheum* 2011;63:722–32.
- Ainiala H, Dastidar P, Loukkola J *et al.* Cerebral MRI abnormalities and their association with neuropsychiatric manifestations in SLE: a population-based study. *Scand J Rheumatol* 2005;34:376–82.
- Kozora E, Filley CM. Cognitive dysfunction and white matter abnormalities in systemic lupus erythematosus. *J Int Neuropsychol Soc* 2011;17:385–92.
- Inglese F, Kant IMJ, Monahan RC *et al.* Different phenotypes of neuropsychiatric systemic lupus erythematosus are related to a distinct pattern of structural changes on brain MRI. *Eur Radiol.* 2021;31:8208–10.
- De Bresser J, Kuijff HJ, Zaanen K *et al.* White matter hyperintensity shape and location feature analysis on brain MRI; Proof of principle study in patients with diabetes. *Sci Rep* 2018;8:1893.
- Kant IMJ, de Bresser J, van Montfort SJT *et al.* Preoperative brain MRI features and occurrence of postoperative delirium. *J Psychosom Res* 2021;140:110301.
- Kant IMJ, Mutsaerts HJMM, van Montfort SJT *et al.* The association between frailty and MRI features of cerebral small vessel disease. *Sci Rep* 2019;9:11343.
- Ghaznawi R, Geerlings MI, Jaarsma-coes MG *et al.* The association between lacunes and white matter hyperintensity features on MRI: The SMART-MR study. *J Cereb Blood Flow Metab* 2019;39:2486–96.
- Ghaznawi R, Geerlings M, Jaarsma-Coes M, Hendrikse J, de Bresser J on behalf of the UCC-Smart

- Study Group. Association of white matter hyperintensity markers on MRI and long-term risk of mortality and ischemic stroke. *Neurology* 2021;96:e2172–83.
- 18 Hanly JG, Urowitz MB, Sanchez-Guerrero J *et al.* Neuropsychiatric events at the time of diagnosis of systemic lupus erythematosus: an international inception cohort study. *Arthritis Rheum* 2007;56:265–73.
 - 19 Bortoluzzi A, Scirè CA, Bombardieri S *et al.* Development and validation of a new algorithm for attribution of neuropsychiatric events in systemic lupus erythematosus. *Rheumatol* 2014;54:891–8.
 - 20 Hanly JG. Diagnosis and management of neuropsychiatric SLE. *Nat Rev Rheumatol* 2014;10:338–47.
 - 21 Magro-Checa C, Zirkzee EJ, Huizinga TW, Steup-Beekman GM. Management of neuropsychiatric systemic lupus erythematosus: current approaches and future perspectives. *Drugs* 2016;76:459–83.
 - 22 Monahan RC, Fronczek R, Eikenboom J *et al.* Mortality in patients with systemic lupus erythematosus and neuropsychiatric involvement: a retrospective analysis from a tertiary referral center in the Netherlands. *Lupus* 2020;29:1892–901.
 - 23 Gladman DD, Ibañez D, Urowitz MB. Systemic lupus erythematosus disease activity index 2000. *J Rheumatol* 2002;29:288–91.
 - 24 Gladman DD, Goldsmith CH, Urowitz MB *et al.* The Systemic Lupus International Collaborating Clinics/ American College of Rheumatology (SLICC/ACR) Damage Index for systemic lupus erythematosus international comparison. *J Rheumatol* 2000;27:373–6.
 - 25 Jenkinson M, Smith S. A global optimisation method for robust affine registration of brain images. *Med Image Anal* 2001;5:143–56.
 - 26 Jenkinson M, Bannister P, Brady M, Smith S. Improved optimization for the robust and accurate linear registration and motion correction of brain images. *Neuroimage* 2002;17:825–41.
 - 27 Kant IMJ, de Bresser J, van Montfort SJT *et al.* The association between brain volume, cortical brain infarcts, and physical frailty. *Neurobiol Aging* 2018;70:247–53.
 - 28 Griffanti L, Jenkinson M, Suri S *et al.* Classification and characterization of periventricular and deep white matter hyperintensities on MRI: a study in older adults. *NeuroImage* 2018;170:174–81.
 - 29 Ramirez GA, Rocca MA, Preziosa P *et al.* Quantitative MRI adds to neuropsychiatric lupus diagnostics. *Rheumatology* 2021;60:3278–88.
 - 30 Heinen R, Steenwijk MD, Barkhof F *et al.* Performance of five automated white matter hyperintensity segmentation methods in a multicenter dataset. *Sci Rep* 2019;9:16742.
 - 31 Mendrik AM, Vincken KL, Kuijf HJ *et al.* MRBrainS challenge: online evaluation framework for brain image segmentation in 3T MRI scans. *Comput Intell Neurosci* 2015;2015:813696.